

Simulation of large wind pressures by gusts on a bluff structure

Seung-Hwan Jeong[†]

Department of Civil Engineering, Yonsei University, Seoul 120-749, Korea
(Received May 24, 2003, Accepted July 30, 2004)

Abstract. This paper illustrates application of the proper orthogonal decomposition (POD) and the autoregressive (AR) model to simulate large wind pressures due to gusts on a low-rise building. In the POD analysis, the covariance of the ensemble of large wind pressures is employed to calculate the principal modes and coordinates. The POD principal coordinates are modeled using the AR process, and the fitted AR models are employed to generate the principal coordinates. The generated principal coordinates are then used to simulate large wind pressures. The results show that the structure characterizing large wind pressures is well represented by the dominant eigenmodes (up to the first fifteen eigenmodes). Also, wind pressures with large peak values are simulated very well using the dominant eigenmodes along with the principal coordinates generated by the AR models.

Keywords: proper orthogonal decomposition; autoregressive model; large wind pressure; pressure simulation.

1. Introduction

Characteristics of gusts and wind-induced large pressures on buildings and structures are of considerable interest in wind engineering. The gust peak values are important in determining the dynamic response of buildings and structures, and endeavors to investigate strong gusts and their effects on buildings and structures have been made in wind and civil engineering applications (Solari and Repetto 2002, Xu and Guo 2003). It has been recognized in turbulence research that the extreme temporal fluctuations of aerodynamic loading are associated with organized, large coherent structures in flow. The proper orthogonal decomposition (POD) is a noble tool developed for the analysis of coherent structures in the random field of turbulence. Armit (1968) first applied the POD in wind engineering to analyze wind pressure on a bluff body. Panofsky and Dutton (1984) produced simulated strong gusts using the random samples of the POD principal coordinates. Recently, the POD was applied in the investigation of wind-induced pressure on buildings (Bienkiewicz, *et al.* 1995, Tamura, *et al.* 1999) and the vibration analysis of structural systems (Azeez and Vakakis 2001).

The autoregressive (AR) model provides a statistical representation of uniformly sampled time series by a finite number of parameters. The AR process, Brockwell and Davis (1991), has been successfully employed in the field of wind engineering to investigate approaching wind and wind-induced loading on buildings and structures. Scanlan and Fortier (1982) used the AR process to

[†] Research Associate

model the full-scale data of wind velocity and wind pressure signals on a cooling tower. Stathopoulos and Mohammadian (1991) fitted the AR model for roof pressure obtained during wind-tunnel studies. Li and Kareem (1990) considered the AR process in development of efficient simulation techniques for studies of wind effects. Jeong and Bienkiewicz (1997) also investigated wind-induced pressure on a low-rise building and found a relatively low order AR model to be appropriate for the considered wind pressure and its dominant POD principal coordinates. Fang, *et al.* (1999) investigated damping values in a building, obtained from field measurements, and established the AR model of damping.

In this paper, the POD is employed to identify the coherent structure of large wind pressures due to gusts. The roof pressure obtained from a field study of the TTU test building is used in the analysis. A collection of large wind pressures is extracted from the pressure data, and then the POD is applied to the ensemble of large wind pressures constructed with the peak pressure at the midpoint of the time interval. The covariance matrix of the ensemble is employed to calculate the principal modes and coordinates. Next, the AR models are fitted for the POD principal coordinates, and the fitted AR models are employed to generate the new principal coordinates. The POD modes and the generated principal coordinates are used to simulate wind pressures with large peak values.

2. Background

2.1. Proper orthogonal decomposition (POD) analysis

The objective of the POD is to find a deterministic function that is similar to all the elements of the ensemble of a random field. Given a random pressure $p(y, t)$, the maximum of the projection of $p(y, t)$ on a deterministic function $\Psi(t)$ can be found. Implementation of this condition in the mean-square sense leads to the following condition.

$$\int R_p(t, t') \Psi(t') dt' = \lambda \Psi(t) \quad (1)$$

where $R_p(t, t')$ is the covariance of pressure time series. The solutions of the above eigenvalue problem, the eigenvalues λ and the eigenfunctions $\Psi(t)$, provide the basis for the POD. The random pressure $p(y, t)$ can be represented as a series expansion:

$$p(y, t) = \sum_k a_k(y) \Psi_k(t) \quad (2)$$

where the principal coordinates are

$$a_k(y) = \int p(y, t) \Psi_k(t) dt \quad (3)$$

The principal coordinates $a_k(y)$ are statistical and vary with each pressure time series in the random pressure field. The eigenfunctions $\Psi_k(t)$ are deterministic and represent the integrated temporal dependence of the entire random pressure field.

2.2. Autoregressive (AR) process

A series $a(y)$ having a zero mean is an autoregressive process of order m , denoted as AR(m), if it

is stationary and satisfies the difference equation

$$a(y) = \phi_1 a(y-1) + \phi_2 a(y-2) + \dots + \phi_m a(y-m) + \varepsilon(y) \quad (4)$$

where ϕ_1, \dots, ϕ_m are the AR coefficients and $\varepsilon(y)$ is a white noise process with zero mean and variance σ_ε^2 . The model parameters are related to the autocorrelation function (ACF) and the partial autocorrelation function (PACF). For a given lag, the ACF is the measure of the dependence between two observations, while the PACF expresses the dependence between the residuals of the two observations, which result from the removal of the effect of the intervening observations. The PACF is the m^{th} autoregressive coefficient in the AR model of order m . For AR models, the PACF is of main interest. As an initial guess, the model order m is assumed equal to the lag number beyond which the magnitude of the PACF is negligible. Next, the model parameters $\phi_i, i = 1, \dots, m$, are estimated. Initial prediction of the parameters, typically made for AR models using the Yule-Walker equations, can be subsequently refined using a number of approaches, including the least squares and maximum likelihood methods, Brockwell and Davis (1991).

The model order is optimized to determine the best order without overfitting the model. The effectiveness of these modifications is typically assessed by monitoring the decrease in the variance of residuals (discrepancy between the series and the fitted model) as the model order is increased. Criteria used in this process include the final prediction error (FPE), the bias corrected version of the Akaike Information Criterion (AICC), and the Bayesian Information Criterion (BIC). In the paper, the FPE is used in optimizing the order of AR models. The FPE for AR models, after Brockwell and Davis (1991), reads as follows

$$FPE = \hat{\sigma}_\varepsilon^2 \frac{n+m}{n-m} \quad (5)$$

where $\hat{\sigma}_\varepsilon^2$ is the maximum likelihood estimate of σ_ε^2 and n is the number of observations.

Validation of the fitted model is accomplished through examining the residuals and comparing the model and sample ACF. The residuals are defined as follows

$$\hat{r}_y = (a(y) - \hat{a}(y)) / \sqrt{E(a(y) - \hat{a}(y))^2 / \sigma_\varepsilon^2} \quad (6)$$

where $\hat{a}(y)$ is the predicted value of $a(y)$ based on observations up to point $y-1$, σ_ε^2 is the white noise variance of the fitted model, and E is the expectation operator. The residuals should resemble a realization of a white noise sequence. This property is verified by inspecting the ACF of the residuals. The goodness of fit of the model is also examined by using a number of tests. In this paper, the residual correlation-based McLeod-Li Portmanteau (MLP) test, Brockwell and Davis (1991), is employed. The MLP test statistic is defined by

$$MLP = n(n+2) \sum_{j=1}^h \hat{\rho}_{rr}^2(j) / (n-j) \quad (7)$$

where $\hat{\rho}_{rr}(j)$ is the sample autocorrelations of the squared residuals at lag j and h is the maximum number of lags. If the model is correctly fitted, then MLP is approximately chi-squared with h degrees of freedom. The adequacy of the proposed model is rejected at level α if the value of MLP is larger than the $(1-\alpha)$ quantile of the chi-square distribution.

3. Results and discussion

The time series of wind-induced pressure used in the paper was obtained from a field study of the Texas Tech University test building, as Fig. 1 shows. The point pressure at a representative location (tap 50501) on the roof corner of the building was measured for the wind direction $\theta = 223^\circ$, as depicted in Fig. 1. Fig. 2 shows a sequence of 36000 samples of pressure acquired at a sampling rate of 40 Hz.

In the paper, a collection consisting of 99 pressure time series with negative peak values stronger

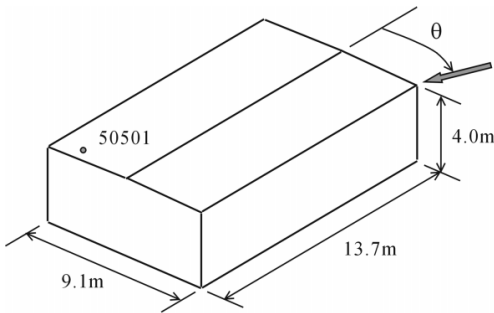


Fig. 1 TTU test building

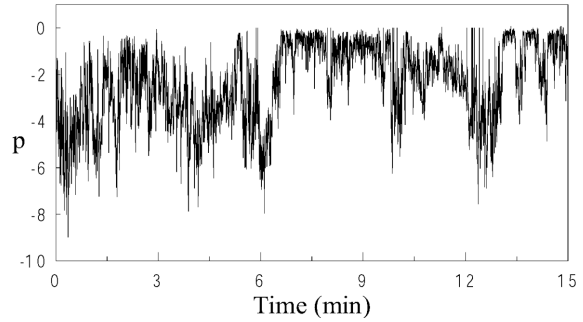


Fig. 2 Original wind pressure

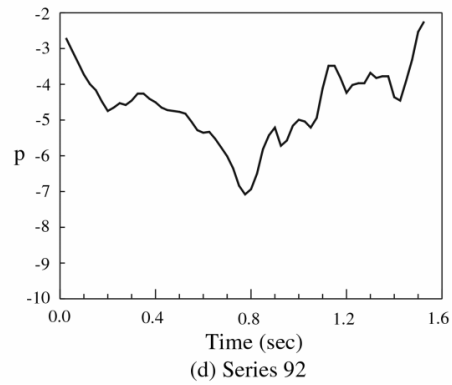
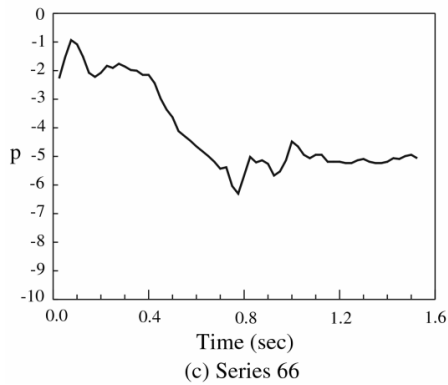
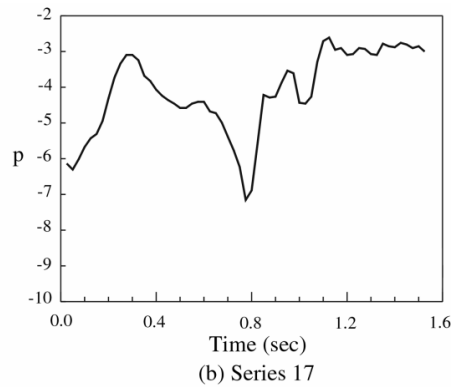
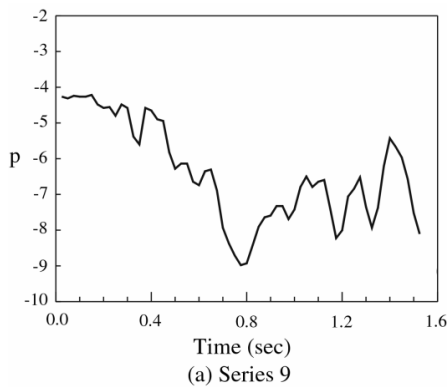


Fig. 3 Representative pressure time series

than the pressure coefficient of -5.2 was extracted from the original pressure data in Fig. 2. Then an ensemble of large wind pressures was constructed with the negative peak pressure at the midpoint of the time interval. Fig. 3 shows four representative time series among the 99 records of wind pressure extracted from the original data. The POD was applied to the ensemble of large wind pressures after subtracting the mean of the original data.

The representative results of the POD analysis are presented in Table 1 and Fig. 4. It is shown in

Table 1 First ten and subsequent representative eigenvalues

| Mode k | Eigenvalue λ_k | Proportion (%) $\lambda_k / \sum_n \lambda_n$ | Cumulative proportion (%) |
|-------------|---------------------------|--|---------------------------|
| 1 | 385.23 | 92.87 | 92.87 |
| 2 | 9.24 | 2.23 | 95.10 |
| 3 | 5.89 | 1.42 | 96.52 |
| 4 | 3.21 | 0.77 | 97.29 |
| 5 | 2.63 | 0.63 | 97.93 |
| 6 | 1.61 | 0.39 | 98.31 |
| 7 | 1.24 | 0.30 | 98.61 |
| 8 | 0.90 | 0.22 | 98.83 |
| 9 | 0.75 | 0.18 | 99.01 |
| 10 | 0.53 | 0.13 | 99.14 |
| 20 | 0.12 | 0.03 | 99.80 |
| 30 | 0.03 | 0.01 | 99.95 |
| 60 | 0.00 | 0.00 | 100.00 |

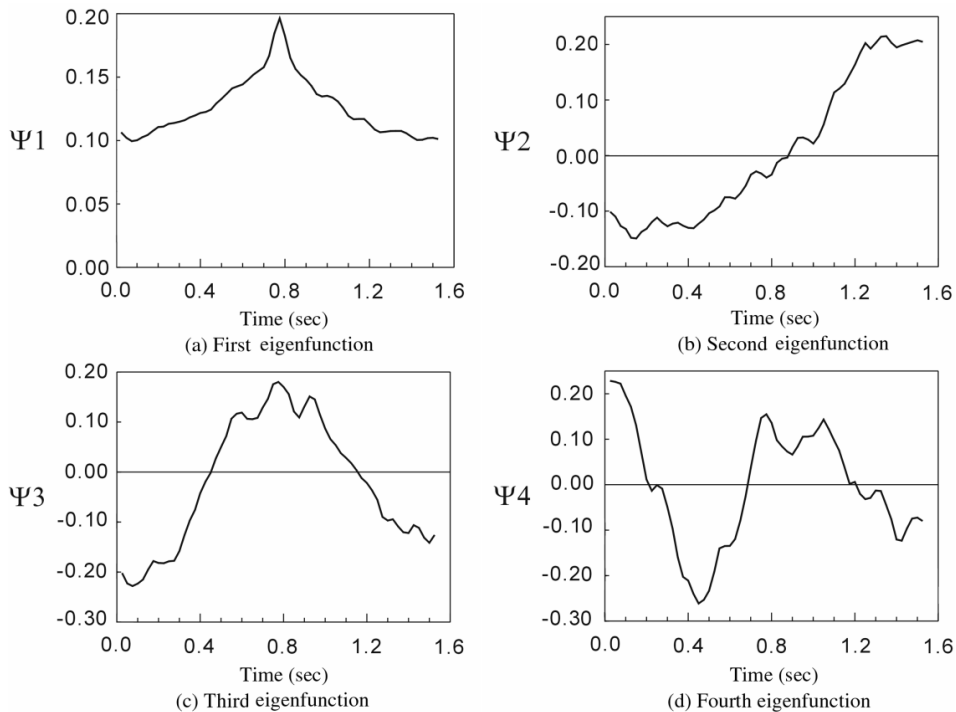


Fig. 4 Eigenfunctions of pressure

Table 2 Statistical properties of the first ten principal coordinates

| Mode k | Mean $\langle a_k \rangle$ | Standard deviation σ_k | Mode k | Mean $\langle a_k \rangle$ | Standard deviation σ_k |
|-------------|-------------------------------|----------------------------------|-------------|-------------------------------|----------------------------------|
| 1 | -18.71 | 5.93 | 6 | -0.10 | 1.27 |
| 2 | 0.04 | 3.04 | 7 | -0.05 | 1.11 |
| 3 | -0.34 | 2.40 | 8 | -0.05 | 0.95 |
| 4 | -0.16 | 1.78 | 9 | 0.00 | 0.87 |
| 5 | 0.10 | 1.62 | 10 | -0.03 | 0.73 |

Table 1 that the first eigenvalue is significantly greater in magnitude than the other eigenvalues. The first four eigenfunctions (modes) of the pressure are depicted in Fig. 4. The first mode exhibits the largest value at the midpoint of the time interval, which implies that the largest value makes a significant contribution to identifying the structure of large wind pressures due to gusts. The means and standard deviations of the first ten principal coordinates computed from the POD analysis are listed in Table 2. It is shown that the first principal coordinate takes a significantly larger negative mean value compared to the remaining coordinates.

The POD results can be used to reconstruct the original large wind pressure using the modal expansion defined by Eq. (2). Fig. 5 depicts a convergence of the reconstructed pressure to the original pressure with the largest negative peak (series 9, Fig. 3) for an increasing number of modes.

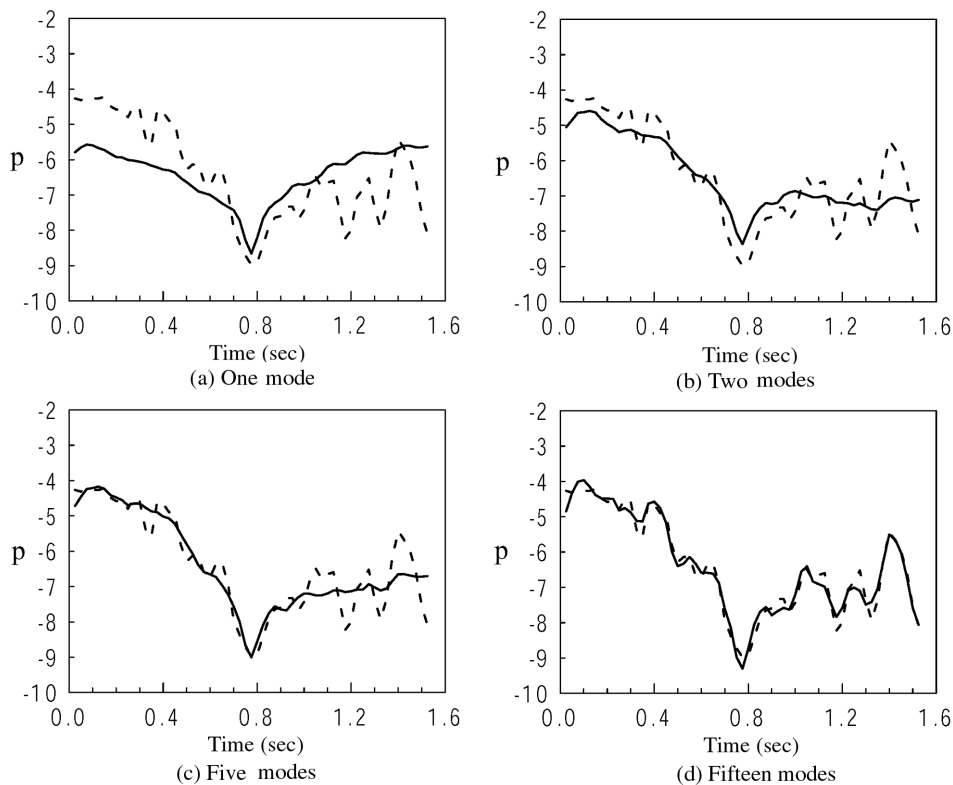


Fig. 5 Original (---) and reconstructed (—) pressure using (a) one, (b) two, (c) five and (d) fifteen modes

The effect of the number of modes on the reconstruction error is illustrated in Fig. 6. The reconstruction error is defined as the root mean square value of the difference between the original and reconstructed pressure divided by the original pressure. It can be seen that the error is lower than 3% when the first fifteen (approximately 25% of all the modes) or more modes are considered.

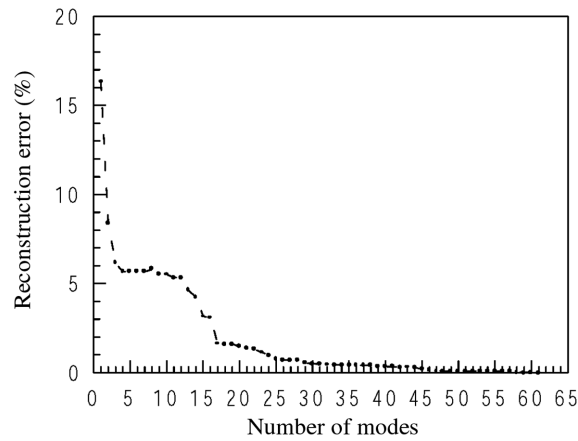


Fig. 6 Reconstruction error

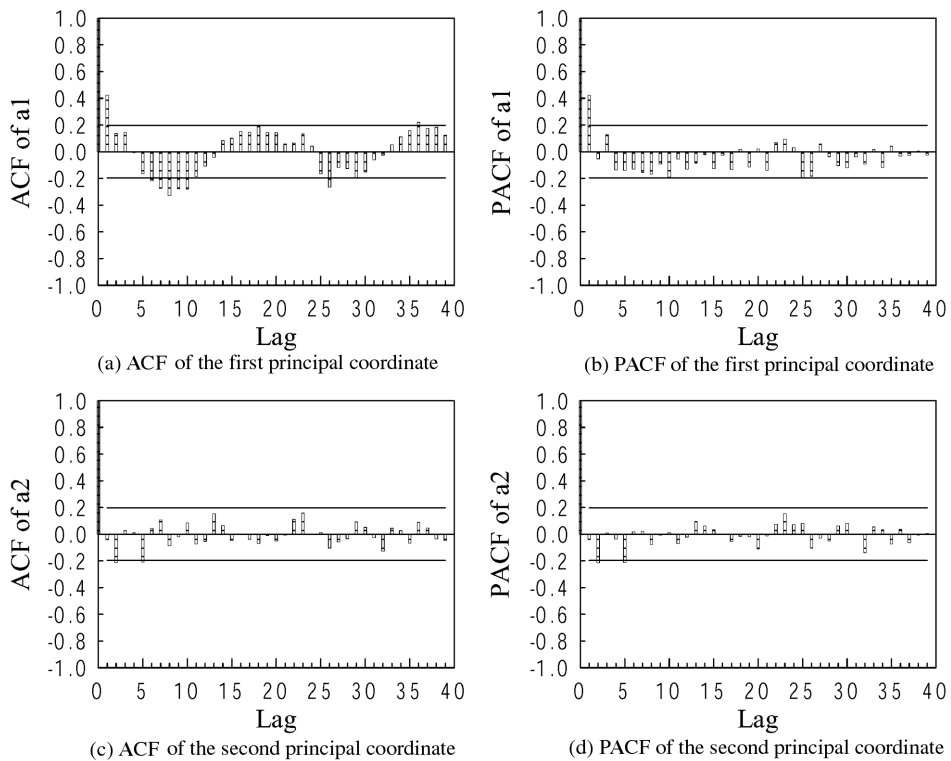


Fig. 7 (a) ACF and (b) PACF of the first principal coordinate, and (c) ACF and (d) PACF of the second principal coordinate

The AR model was next applied to the principal coordinates. Matching of the model was accomplished by using the program ITSM, Brockwell and Davis (1991). The autocorrelation function (ACF) and the partial autocorrelation function (PACF) are shown for the first two principal coordinates in Fig. 7. The horizontal lines on the graph display the approximate 95% bounds for the autocorrelations of a white noise sequence. The PACF value for the first principal coordinate is large at lag 1, which suggests an AR model of low order. The ACF and PACF of the second principal coordinate appear to be those of a white noise sequence.

Preliminary estimate of the AR-model parameters was made using the Yule-Walker equations, but the final decision of the parameters was based on the more refined maximum likelihood method. The final prediction error (FPE) was employed in optimization of the model order. Fig. 8 shows the FPE value as a function of the model order m for the first two principal coordinates. The AR order m associated with the minimum FPE was selected as an optimal order. As shown in Fig. 8 and Table 3, the AR orders for the first and the second principal coordinates are, respectively, 10 and 2, based on the FPE. The minimum-FPE AR models of order 10 with zero coefficients except at lags 1, 2, 3, 5, 8 and 10 was selected as the best-fitting model for the first principal coordinate. The selected AR(10) model is expressed as

$$a(y) = 0.345a(y - 1) - 0.156a(y - 2) + 0.084a(y - 3) - 0.159a(y - 5) - 0.214a(y - 8) - 0.265a(y - 10) + \varepsilon(y) \tag{8}$$

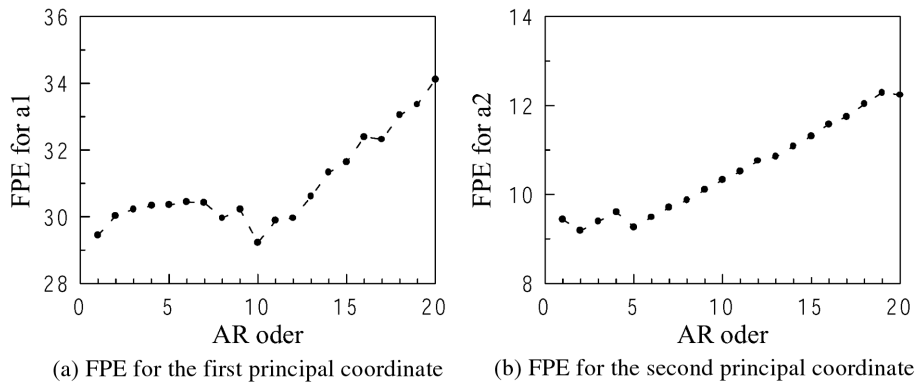


Fig. 8 FPE for the (a) first and (b) second principal coordinate

Table 3 AR order for the first five principal coordinates

| Principal Coordinates | AR order m | AR coefficients $\phi_i, i=1, \dots, m$ | White noise variance | Min. FPE | MLP test (df=26, $\chi^2_{0.95} = 38.9$) | AR order for residuals |
|-----------------------|--------------|--|----------------------|----------|---|------------------------|
| a_1 | 10 | 0.345, -0.156, 0.084, 0, -0.159, 0, 0, -0.214, 0, -0.265 | 23.728 | 27.24 | 13.5 | 0 |
| a_2 | 2 | 0, -0.218 | 8.795 | 9.00 | 21.7 | 0 |
| a_3 | 0 | - | 3.457 | - | 32.2 | 0 |
| a_4 | 3 | 0, -0.179, 0.202 | 2.946 | 3.09 | 24.2 | 0 |
| a_5 | 0 | - | 1.910 | - | 19.3 | 0 |

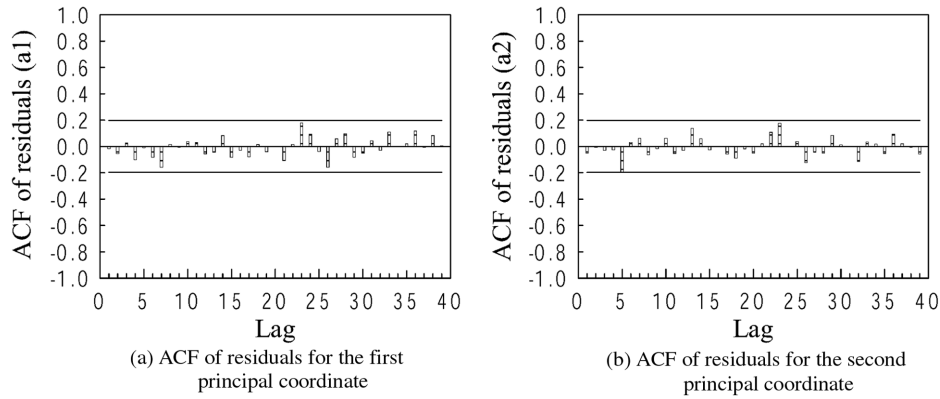


Fig. 9 ACF of AR model residuals for the (a) first and (b) second principal coordinate

where $\varepsilon(y)$ is a sequence of uncorrelated random variables with mean 0 and variance 23.728. Table 3 shows that the AR orders for the third and fifth coordinates are zero, which means that there are no correlations outside the bounds for the autocorrelations of a white noise sequence.

The ACF of the residuals and the MLP test statistics were employed to check whether the model was correctly fitted. The ACF of the residuals is depicted in Fig. 9 for the first two principal coordinates and appears to be compatible with the hypothesis that the residuals constitute a white noise sequence. As shown in Table 3, the results of the MLP test indicate a good fit of the AR models. The AR order for the residuals of each principal coordinate, Table 3, is zero, which suggests that no correlations remain in the residuals. The ACF and PACF of the original first principal coordinate are compared with those of the modeled coordinate in Fig. 10. The comparisons show that the ACF and PACF of the original principal coordinate are similar to the model ACF and PACF.

The new principal coordinates were generated using the applied AR models with normally distributed random variables. The data points of each principal coordinate generated from the AR model were 200, which were approximately twice those of the original coordinate computed from the POD analysis. The ACF and PACF of the generated first principal coordinate shown in Fig. 11 look compatible with those of the modeled coordinate in Fig. 10.

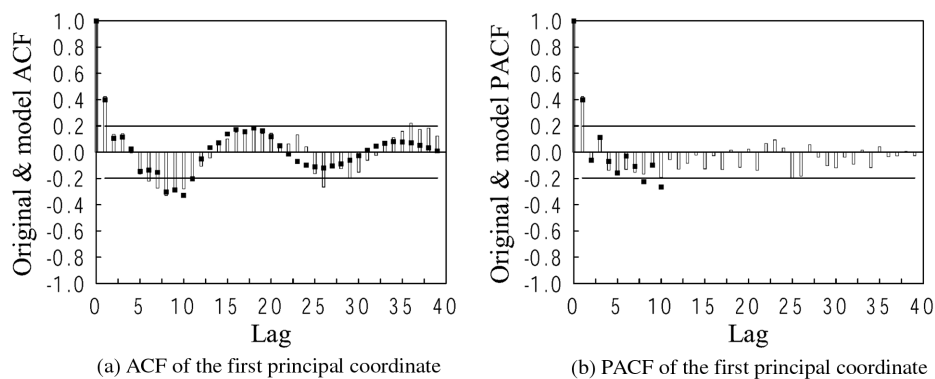


Fig. 10 (a) ACF and (b) PACF of the first principal coordinate: original (||) and model (■)

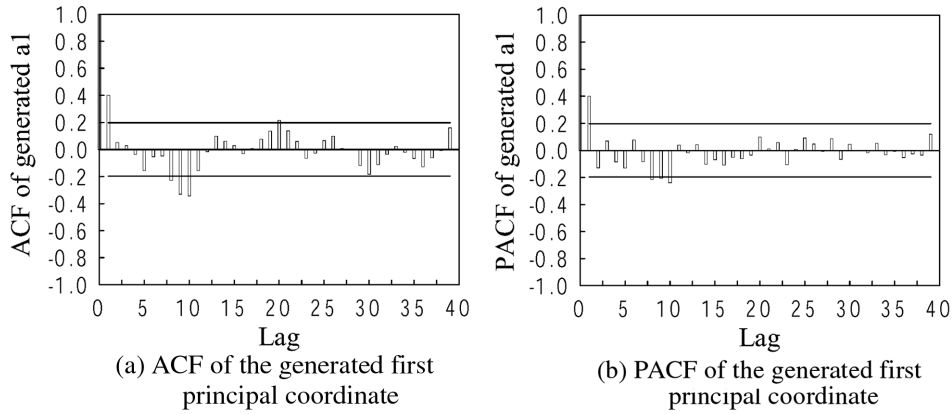


Fig. 11 (a) ACF and (b) PACF of the generated first principal coordinate

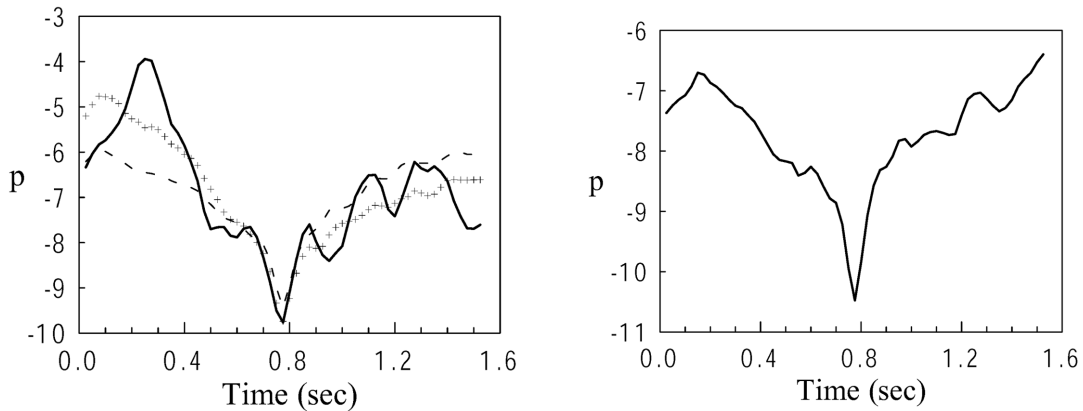


Fig. 12 Simulated large peak pressure using one (---), three (+ +) and fifteen (-) modes

Fig. 13 Simulated large wind pressure with the peak of -10.475 using fifteen modes

The POD modes and the generated principal coordinates were then used to simulate large wind pressures due to gusts employing Eq. (2). Fig. 12 shows the simulated wind pressure for an increasing number of modes. In order to obtain a strong negative peak of wind pressure, the largest value of the first principal coordinate and ordinary values of the other coordinates were used. As a result, wind pressure with a strong negative peak value of -9.764 was produced using the first fifteen eigenmodes, as depicted in Fig. 12. Fig. 13 shows another strong peak value of -10.475, which was produced using the first fifteen eigenmodes and the principal coordinates generated using the AR models with new random variables. The pressure time series 9 in Fig. 3 exhibits the largest negative peak value of -8.979 among the 99 records of wind pressure. It can be seen that the large negative peak of the simulated pressure with the fifteen modes in Figs. 12 and 13 respectively is stronger than the largest peak of the original pressure time series 9 in Fig. 3. The presented data show that wind pressures with large peak values can be produced well using the dominant POD modes and the principal coordinates generated by the AR models.

4. Conclusions

The proper orthogonal decomposition and the autoregressive process were applied to simulate wind pressures with large peak values on a low-rise building. In the POD analysis, the covariance of the ensemble of large wind pressures was employed to calculate the principal modes and coordinates. It was shown that approximately 25% of the modes were required to reconstruct large wind pressure with the error of 3%.

The POD principal coordinates were modeled using the AR process. It was found that, compared to the order of the AR model established for the first principal coordinate, the order of the AR model required for the remaining coordinates was low. The fitted AR models were employed to generate the new principal coordinates. It was shown that wind pressure with the large negative peak, which is stronger than the largest peak of the original random pressure field and characterizes the large wind pressures of the field, was produced using the dominant POD modes (up to the first fifteen eigenmodes) and the generated principal coordinates. Based on the presented study, it is concluded that wind pressures with large peak values can be produced using the dominant POD modes and the principal coordinates generated by the AR models.

Acknowledgements

The author would like to acknowledge the advice of Prof. B. Bienkiewicz of Colorado State University. The experimental data employed in the study was provided by the personnel of WERC, Texas Tech University.

References

- Armitt, J. (1968), "Eigenvector analysis of pressure fluctuations on the West Burton instrumented cooling tower", Internal Report RD/L/N 114/68, Central Electricity Research Laboratories, UK.
- Azeez, M.F.A. and Vakakis, A.F. (2001), "Proper orthogonal decomposition (POD) of a class of vibroimpact oscillations", *J. Sound Vib.*, **240**(5), 859-889.
- Bienkiewicz, B., Tamura, Y., Ham, H.J., Ueda, H. and Hibi, K. (1995), "Proper orthogonal decomposition and reconstruction of multi-channel roof pressure", *J. Wind Eng. Ind. Aerodyn.*, **54/55**, 369-381.
- Brockwell, P.J. and Davis, R.A. (1991), *Time Series: Theory and Methods*, 2nd ed., Springer-Verlag.
- Fang, J.Q., Jeary, A.P., Li, Q.S. and Wong, C.K. (1999), "Random damping in buildings and its AR model", *J. Wind Eng. Ind. Aerodyn.*, **79**, 159-167.
- Jeong, S.H. and Bienkiewicz, B. (1997), "Application of autoregressive modeling in proper orthogonal decomposition of building wind pressure", *J. Wind Eng. Ind. Aerodyn.*, **69-71**, 685-695.
- Li, Y. and Kareem, A. (1990), "ARMA representation of wind field", *J. Wind Eng. Ind. Aerodyn.*, **36**, 415-427.
- Panofsky, H.A. and Dutton, J.A. (1984), *Atmospheric Turbulence: Models and Methods for Engineering Applications*, John Wiley and Sons.
- Scanlan, R.H. and Fortier, L.J. (1982), "Turbulent winds and pressure effects around a rough cylinder at high Reynolds number", *J. Wind Eng. Ind. Aerodyn.*, **9**, 207-236.
- Solari, G. and Repetto, M.P. (2002), "General tendencies and classification of vertical structures under gust buffeting", *J. Wind Eng. Ind. Aerodyn.*, **90**, 1299-1319.
- Stathopoulos, T. and Mohammadian, A.R. (1991), "Modeling of wind pressures on monoslope roofs", *Eng. Struct.*, **13**, 281-292.
- Tamura, Y., Suganuma, S., Kikuchi, H. and Hibi, K. (1999), "Proper orthogonal decomposition of random wind pressure field", *J. Fluids Struct.*, **13**, 1069-1095.

Xu, Y.L. and Guo, W.H. (2003), "Dynamic behaviour of high-sided road vehicles subject to a sudden crosswind gust", *Wind Struct.*, **6**(5), 325-346.

CC